Study on Flow Fields and Aerodynamic Characteristics for Mars Exploration Airplane

Report Number: R22EACA18
Subject Category: JSS Inter-University Research
URL: https://www.jss.jaxa.jp/en/ar/e2022/20749/

Responsible Representative

Seiichiro Morizawa, Lecturer, National Institute of Technology, Okinawa College

Contact Information

Seiichiro Morizawa(morizawa@okinawa-ct.ac.jp)

Members

Seiichiro Morizawa, Takashi Matsuno

Abstract

Recently, many kinds of research on unmanned aerial vehicles such as the Martian atmosphere and a high altitude one in the Earth's stratosphere have been conducted actively. These environments become that the atmospheric density and temperature are much lower. Then, the flight condition of the airplane is low Reynolds and high Mach numbers condition, and the aerodynamic data is insufficient for designing these vehicles. The purpose of this study is to investigate the relationship between aerodynamic and flow field at the low Reynolds and high Mach numbers condition, and clary the unique fluid phenomena under the condition. In addition, the aerodynamic devices suitable under such the condition are explored.

Reasons and benefits of using JAXA Supercomputer System

The computational cost of parametric CFD studies of 3D geometries is very high. Therefore, the use of JSS3 is indispensable for the computation on large memory and CPUs such as supercomputers.

Achievements of the Year

In this year, the numerical simulations at Mach number of 0.2 (low subsonic flow) and 0.74 (transonic flow) are conducted to see the difference in aerodynamic characteristics between the wing_grid and rectangular wing. The wing_grid is a wingtip device with multiple wingtip bifurcations and gaps that mimic the shape of birds as shown in Fig.1.

Figure 2 shows the aerodynamic coefficients of wing_grid and rectangular wing. As shown in Fig. 2 (a), the coefficient of lift (CL) of the wing_grid with Mach number 0.74 is smaller than that of the rectangular wing at all angles of attack (AoA), and the CL difference between these wings increases as the AoA increases. On the other hand, The CL of wing_grid at Mach number 0.20 was larger than that of these wings at Mach number 0.74 for all angles of attack, and the same trend was observed for the angle of attack at Mach number 0.20.

Next, Fig. 2(b) shows that the coefficient of drag (CD) of the wing_grid with Mach numbers of 0.20 and 0.74 exceeds that of the rectangular wing, and that of the wing_grid with Mach number 0.20 is almost the same at all AoA. The CD of the rectangular wing is close to that of the wing_grid. The CD of the wing_grid increases as the AoA increases, and the CD of the rectangular wing with Mach number of 0.74 is higher than that of the rectangular wing with Mach number of 0.20.

In addition, Fig. 3 shows the pressure coefficient (Cp) distribution against the normalized chordlength direction (x/c) at an AoA of 0 deg. and deg and the Cp distribution against the normalized vertical direction (z/t) at an AoA of 6 deg to further evaluate the effect of the wing_grid. As a result, the wing_grid produces a large Cp at the first stage, although the suction loops after the second stage are missing from Fig. 3(a). On the other hand, Fig. 3(b) shows that only drag loops exist for these wings, and in particular, the drag loops at each stage of the wing_grid are large. In particular, the area of the drag loops in the first and second stages of the wing_grid become larger.

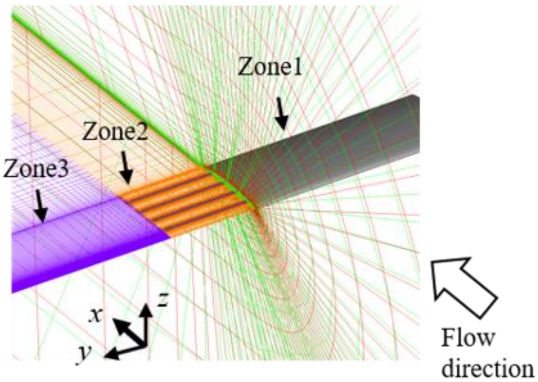

Fig. 1: Computational grid of the wing_grid

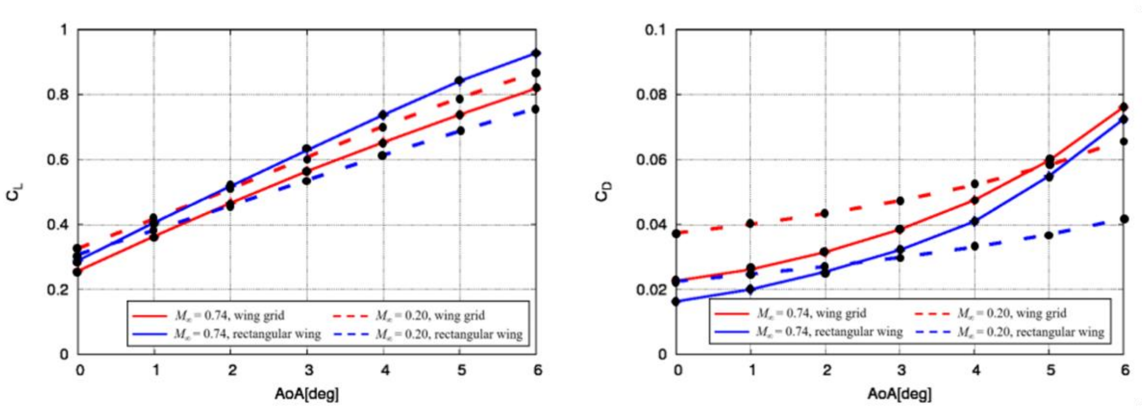

(a) Lift coefficient (b) Drag coefficient

Fig. 2: Aerodynamic coefficients between wing_grid and rectangular wing

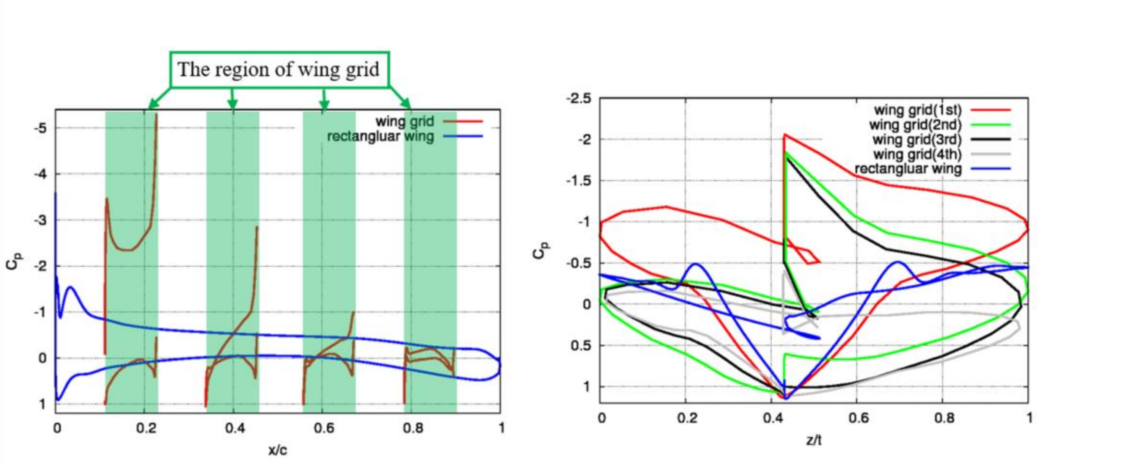

(a)Chord-length direction with AoA of 6° and M_∞ of 0.20 (b)Vertical-length direction with AoA of 0° and M_∞ of 0.74

Fig. 3: Pressure coefficient near wingtip between wing_grid and rectangular wing

Publications

- Peer-reviewed papers

Seiichiro Morizawa, and Shigeru Obayashi, "Investigation of a Planar Wing with Wing Grid using CRM.65.airfoil," Bulletin of National Institute of Technology, Okinawa College, No.16, pp. 61-72, 2022. ISSN:2345-2136.

Usage of JSS

- **Computational Information**

Process Parallelization Methods	N/A
Thread Parallelization Methods	Automatic Parallelization
Number of Processes	1
Elapsed Time per Case	300 Minute(s)

- **JSS3 Resources Used**

Fraction of Usage in Total Resources[*1](%): 0.00

Details

Computational Resources		
System Name	CPU Resources Used (core x hours)	Fraction of Usage[*2](%)
TOKI-SORA	58.67	0.00
TOKI-ST	0.00	0.00
TOKI-GP	0.00	0.00
TOKI-XM	0.00	0.00
TOKI-LM	0.00	0.00
TOKI-TST	0.00	0.00
TOKI-TGP	0.00	0.00
TOKI-TLM	0.00	0.00

File System Resources		
File System Name	Storage Assigned (GiB)	Fraction of Usage[*2] (%)
/home	169.17	0.15
/data and /data2	3,438.33	0.03
/ssd	58.33	0.01

Archiver Resources		
Archiver Name	Storage Used (TiB)	Fraction of Usage[*2] (%)
J-SPACE	0.00	0.00

[*1]: Fraction of Usage in Total Resources: Weighted average of three resource types (Computing, File System, and Archiver).

[*2]: Fraction of Usage：Percentage of usage relative to each resource used in one year.

- **ISV Software Licenses Used**

ISV Software Licenses Resources		
	ISV Software Licenses Used (Hours)	Fraction of Usage[*2] (%)
ISV Software Licenses (Total)	0.00	0.00

[*2]: Fraction of Usage：Percentage of usage relative to each resource used in one year.